3D Front Face fluorescence Spectroscopy as a tool for monitoring the oxidation level of edible vegetable oil during storage at 60 °C

Eliot Patrick BOTOSOA[a], Romdhane KAROUI[a,b]*

[a]Univ. Artois, Univ. Lille, Univ. Littoral Côte d'Opale, Univ. Picardie Jules Verne, Univ. de Liège, INRAE, Junia, UMR-T 1158, BioEcoAgro, F-62300 Lens, France

[b]ADRIANOR, F-62217, Tilloy Les Mofflaines, France

*Correspondence author: Romdhane Karoui

Tel: +33 3 21 79 17 00; Fax: +33 3 21 79 17 17

Email: romdhane.karoui@univ-artois.fr

Abstract

Fluorescence landscapes with excitation wavelengths varying between 280 and 400 nm, and emission wavelengths in the range of 300 – 650 nm were scanned directly on oil samples throughout storage in capped and uncapped flasks for 15 days at 60 °C. PARAFAC analysis of the fluorescence landscapes showed the presence of three fluorophores in the edible oils, which are strongly dependent on the storage conditions. The fluorescence spectra were resolved into excitation and emission profiles of the pure fluorescent compounds, which are ascribed to be oxidation products and vitamin E. The complexity of edible oil data sets was suitable for PARAFAC modeling. Problems with scattering were encountered, the use of missing values was tackled before obtaining a validated model with a criterion of similarity measurements of splits reaching the 83.8 % and this allowed us to start getting through the model of interpretation.

Keywords: Vegetable oil; Thermo-oxidation; Fluorescence spectroscopy; excitation-emission matrix; PARAFAC.

41 -

42 ## 1. Introduction

43

44 World trends in oil crop production, yield, and growing area over the last 30 years exhibited
45 an increase of 240 %, 82 %, and 48 %, respectively (El-Hamidi & Zaher, 2018).
46 Consequently, the food industry will be faced with challenges to set up reliable and robust
47 methods in the evaluation of edible oils quality during the process and/or storage. Several
48 chemical reactions contribute to the chemical, physical and sensorial aging of edible oils.
49 During heating, edible oils undergo degradation and their functional and organoleptic features
50 are significantly modified. The heating induces chemical reactions such as oxidation,
51 polymerization, hydrolysis and cis/trans isomerization, which have a huge impact not only on
52 the nutritional value of oils but may also generate toxic compounds damaging to health
53 (Schaich, 2013). Oxidation stability is considered one of the most important quality indicators
54 of edible vegetable oils. It determines their usefulness in technological processes as well as
55 shelf life. Several methods enable to determine the oxidative stability of oils. The most
56 reliable one is the aging test at ambient temperature that requires a long time (several
57 months). Therefore, methods that allow the determination of oil stability in the shortest
58 possible time are valuable such as Schaal oven test, swift test or AOM (Active Oxygen
59 Method), Rancimat test, Oxidograph, Oxipress, and Rapidoxy. The Schaal oven test is one of
60 the most frequently used accelerated shelf life of edible oils. This accelerated oxidation test
61 consists of storing oil samples at a constant and controlled temperature at ~ 60 °C (Warner,
62 Frankel, & Mounts, 1989). The increase in temperature acts as a gesture and allows oxidation
63 reactions, as well as measuring their evolution, both organoleptically (color, smell, taste) and
64 by chemical analyses. The Schaal oven test has some advantages such as its simplicity and its
65 standardization among the methods referenced in the AOCS database. The oxidation, thermal

stability, chemical composition, and quality of edible oils under various conditions have been previously investigated by applying different techniques such as infrared and Raman spectroscopy (Saleem et al., 2020), 1D and 2D NMR (Cordella, Tekye, Rutledge, & Leardi, 2012; Dugo et al., 2015), differential scanning calorimetry (Qi et al., 2016) and front face fluorescence spectroscopy (FFFS) (Cordella et al., 2012, Ali, Iqbal, Atta, Ullah, & Khan, 2020). Despite of the current progress in the development of these analytical methods; sensory evaluation, chemical analyses (determination of free acidity, acid value, peroxide value, p-anisidine value, totox, thiobarbituric acid (TBA), iodine value) and chromatographic techniques remained the reference methods used in the different regulations such as AFNOR, ISO, and AOCS recommended practice, in edible oil quality control applied during process and storage. These methods are often time-consuming, and require qualified operators. Moreover, chemical analyses and the use of liquid chromatography are incompatible with a reagent and/or organic solvent-free strategy. Indeed, these analyses are performed to get informations from the use of different markers for monitoring the edible oil oxidation state. Each marker provides partial information of the whole phenomenon, but is unable to predict by itself the future stability of the edible oil (Cuvelier and Maillard, 2012). In real-world application, these limitations present some constraints from industrial point of view such as duration, cost and environmental impact of analyses that should be overcome. It would be economically and environmentally profitable and viable to find a promising alternative, which is more compatible with the current state of the art in tehnological development. Many food fluorophores can be used as marker for monitoring the quality of edible oil throughout storage (Sikorska, Khmelinskii, & Sikorski, 2019a). Thus the development of FFFS instruments, methods of data analysis, and availability of suitable software should promote wider usage of fluorescence in food research and real-world application.

Although FFFS is a method, which has been exploited extensively for monitoring food quality (Hassoun & karoui, 2016; Karoui, Cartaud, & Dufour, 2006; Karoui, Hammami, Rouissi, & Blecker 2011; Karoui, Nicolaï, & de Baedemaeker, 2008; Ullah, Khan, Shah, Ali, & Bilal, 2018; Ullah, Khan, Bilal, Ali, & Khalil, 2019), this non-destructive technique has not been fully explored in the determination of the quality of oil products and the comprehension of physico-chemical interactions of lipids with other component occurring within food matrices during storage. In line with this objective, FFFS was used, for instance, to monitor changes in sponge cakes during aging (Botosoa, Chèné, Karoui, 2013a, 2013b). The technique was, recently, presented among high-potential innovative technologies for food quality evaluation (Sikorska et al., 2019a). In addition to its higher sensitivity and selectivity, its multidimensional character, and its usefulness for studying minor and trace components in complex food matrices, FFFS is benefiting from recent technology development to improve its performance in reducing significantly acquisition time of EEM and monitoring specific fluorophores (NADH or tryptophan) and bioprocesses. Several achievements can be cited in that direction such as replacing photomultiplier tubes (PMT) detectors with charge-coupled device (CCD) ones, using compact portable devices with diode lasers or LEDs for food samples measurements, or more advanced sensor like the filter-based Bio View sensor, and usage of optical light guides (Sikorska et al., 2019a). FFFS provides several analytical informations in a non-destructive manner; in addition, sample treatment (extraction or digestion) is not required. This is in line with the view of green chemistry (Gredilla, Fdez-Ortiz de Vallejuelo, Elejoste, de Diego, & Madariaga, 2016). Moreover, the use of FFFS coupled with chemometric tools presented numerous advantages in terms of going in-depth in the comprehension of physico-chemical interactions between fluorescent molecules and their environment within food samples. Several studies have explored the use of FFFS coupled with multiway data analysis, such as PARAFAC. Concerning food research, PARAFAC was

applied in investigating the relationship between sugar impurities and its quality at the molecular level (Bro, 1999), screening method for dioxin contamination in fish oil (Pedersen, Munck, & Engelsen, 2002), monitoring chemical changes in dry-cured Parma ham during maturation (Moller, Parolari, Gabba, Christensen, & Skibsted, 2003), and the stability of processed cheese, yogurt (Christensen, Miquel Becker, & Frederiksen, 2005), and edible oils during storage (Guimet, Ferré, Boqué, Vidal, & Garcia, 2005; Christensen, Nørgaard, Bro, & Engelsen, 2006; Sikorska et al., 2019b).

To the best of our knowledge, up to date; no research study was conducted to determine the oxidative stability of the following four selected vegetable edible oils together, namely rapeseed oil (RO), linseed oil (LO), sunflower oil (SO), and extra virgin olive oil (EVOO) by using 3D Fluorescence spectroscopy coupled with PARAFAC. Due to its importance in the human diet, olive oil (OO) was the most studied in understanding the chemical changes undergone after thermal oxidation (Tena, Aparicio, & García-González, 2012; Saleem et al., 2017; Domínguez Manzano, Muñoz de la Peña, & Durán Merás, 2019). Recently, Sikorska et al., (2019b) depicted, by applying PARAFAC to EEM, the presence of four fluorophores in cold-pressed rapeseed oil that showed different evolution during storage at ambient room temperatures (18 – 25 °C) for 6 months.

The objective of the present study was to determine the impact of heating at 60 °C for 15 days on the quality of RO, LO, SO, and EVOO. Structural changes were monitored at the molecular level by applying 3D FFFS coupled with PARAFAC.

2. Material and methods

2.1 Oil sampling and oil thermo-oxidation procedure

142 A set of 4 edible oils was purchased from a local supermarket and a local producer (Arras,
143 France). The sample collection included 1 sample of 1L of: i) RO; ii) SO; iii) EVOO, and iiii)
144 unrefined and cold-pressed LO.
145 Oil samples (45 mL) were poured into flasks (VWR-France) of 26 mm in diameter, with the
146 surface-to-volume ratio of 0.47 cm^2 / mL and placed into a convection oven (Air Concept,
147 FIRLABO, Emerainville, France), heated and maintained at 60 °C during experimentation,
148 except the sample aged 0 day (fresh oil). No mechanical stirring was applied during the
149 heating period and the flasks were covered with aluminum foil to avoid photo-oxidation. The
150 dishes were introduced into the oven "with" and "without" lids to compare the impact of the
151 presence of air in the headspace of flasks. The samples were analyzed at 0, 3, 6, 9, 13, and 15
152 day(s). One flask of each oil was taken out of the oven and used for 3D fluorescence
153 spectroscopy analysis.
154
155 **2.2 Fluorescence measurements**
156 Fluorescence spectra were recorded using a Fluoromax-4 spectrofluorimeter (Jobin Yvon,
157 Horiba, NJ, USA). The spectrofluorimeter was equipped with xenon lamp source used to
158 excite fluorescence, excitation and emission monochromators, a photomultiplier (PM) (range
159 200 – 850 nm) used as emission detector to measure the intensity of fluorescence, a
160 thermostated front-face sample-cell holder and the temperature was controlled by a Haake
161 A25, AC 200 temperature controller (Thermo-Scientific, France). The incidence angle of the
162 excitation radiation was set at 60° to ensure that reflected light, scattered radiation and
163 depolarization phenomena were minimized. The sample is illuminated by the photons of
164 excitation (light beam: ~ 3 mm in height and ~ 0.3 mm width) in its center during 2-3
165 minutes. The PM responds to individual photons, and the pulses can be detected as an average
166 signal or counted as individual photons. The PM is useful for low-level light detection due to

its capacity to amplify low-noise and its sensitivity depends on the incident wavelength. Fluorescence intensity is a simultaneous function of the excitation and emission wavelengths. The intensity values of a fluorescence emission spectrum are determined by keeping the excitation wavelength (λex) constant while the emission wavelengths (λem) are scanned. Similarly, the intensity values of a fluorescence excitation spectrum are determined by remaining the λem constant, while the λex are scanned. When measuring several emission spectra at different λex (or vice versa), a three-dimensional fluorescence landscape, the so-called fluorescence excitation-emission matrix (EEM), is obtained. The spectra of oil samples were scanned at ambient temperature in a 10 x 10 mm quartz cuvette for a volume of 3 mL. Raw non-smoothed data were recorded. For every oil samples, an EEM was obtained by measuring the emission spectra from 300 to 650 nm at 1 nm intervals with excitation at every 1 nm from 280 to 400 nm. The measurements started with the highest excitation wavelength and ended with the lowest to minimize the photodecomposition of the oil samples. The three main components of the spectrofluorimeter (lamp, monochromators and PM) are wavelength-dependent, therefore, they cause distorsions in the fluorescence spectra. All spectra were corrected for instrumental distortions in excitation using a rhodamine cell in the reference channel. For correcting the excitation spectra, the output **R** of the PM is directly proportional to the flux of photons emitted by the excited sample. This relationship can be written as $\boldsymbol{R} \propto \boldsymbol{I_0 \varepsilon \phi_f}$, where $\boldsymbol{I_0}$ is the excitation intensity, ε is the molar absorptivity, and ϕ_f is the quantum yield of fluorescence efficiency of the selected fluorophor (i.e. the ratio between the number of photons emitted and the number of photons used to excite the system). However, the quantum efficiency of the detector, the bandwidth of the monochromator, and the transmission efficiency of the monochromator must be taken into account for determining the true emission spectrum. Based on these elements, the dependence of the uncorrected emission spectrum can be expressed as follows

$$\frac{dF}{d\lambda} = \left(\frac{dI}{d\lambda}\right) P_\lambda B_\lambda M_\lambda = \left(\frac{dI}{d\lambda}\right) S_\lambda$$

where $dF / d\lambda$ is the apparent or observed intensity of fluorescence emission at wavelength λ ; $dI / d\lambda$ is the true intensity at λ; $P\lambda$, $B\lambda$, and $M\lambda$ represent the relative quantum efficiency of the PM, the relative bandwidth of the monochromator, and the fraction of light transmitted by the monochromator, respectively, at λ. These last three factors were combined into a single factor in Sλ, which is called spectral sensitivity factor of the monochromator-PM combination. The true emission spectrum $dI / d\lambda$ can be determined from the apparent emission spectrum by dividing each ordinate $dF / d\lambda$ by the corresponding value of Sλ.

2.3 Mathematical analyses of data tables

The fluorescence data of oils can be presented in an *I x J x K* three-way data array, which will be trilinear. The first index *(I)* refers to the samples, the second *(J)* to the emission wavelengths and the third (*K*) to the excitation wavelengths. In order to model these data, PARAFAC was used.

The PARAFAC model can be put in the equation as follow:

$$x_{ijk} = \sum_{f=1}^{F} a_{if} b_{jf} c_{kf} - e_{ijk}$$

$i = 1,\ldots,I;\ j = 1,\ldots,J;\ k = 1,\ldots,K$

where x_{ijk} is the intensity of the *ith* sample at the *jth* variable (emission mode) and at the *kth* variable (excitation mode) a_{if}, b_{jf} and c_{kf} are parameters describing the importance of the sample / variables to each component and the residuals, e_{ijk}, contain the variation not captured by the model (Andersen & Bro, 2003).

The PARAFAC components estimate the signals from the individual fluorophores if the data are approximately low-rank trilinear and when the correct number of components is used. In that case, the scores in a_{if} may be interpreted as the relative concentration of analyte f in sample i. The j-vector b_f with elements b_{jf} ($j = 1, \ldots, J$) is the estimated emission spectrum of this analyte and likewise c_f is the estimated excitation spectrum. However, some mathematical conditions must be fulfilled to allow the decomposition to be unique and to provide meaningful estimates (Andersen & Bro, 2003), namely:

- the uniqueness of the decomposition depending on the linearly independence of the spectra and concentration profiles;
- the assumption of the validity of the additivity and linearity of the signal.

The disturbance of the trilinearity of the data can be caused by the inner-filter effects, which may come from high concentrations, scattering and quenching. Furthermore, uncertain estimates can be created because of the abundance of missing data and spectral similarities. Consequently, chemical interpretation should be done with care. Moreover, PARAFAC model can be validated using fit values, visual assessment of the loadings, residual analysis, core consistency diagnostic, jack-knifing and especially by a split-half analysis.

All analyses of the data in this work were performed with PLS Toolbox 7.9 and 8.0 (Eigenvector Research Inc., Wenatchee, WA, USA) and Matlab version R 2013b (The MathWorks, Natick, MA, USA).

3. Results and discussion

3.1 Analysis of edible vegetable oils fluorescence landscapes

Fig. 1a presents the EEM spectra in the form of a contour map of fresh EVOO as an example. The fluorescence landscapes of four edible vegetable oils namely RO, SO, EVOO and LO are shown in **Figs. 1(b and c)** for capped samples and in **Figs. 1(d and e)** for uncapped ones, during 15 days of storage. For the reason of clarity, the present analysis is focused only on the eight samples that represent the extreme in the experimental plan, i.e. four fresh edible oil samples (RO0, SO0, EVOO0, and LO0) and four uncapped edible oil samples (RO-L15, SO-L15, EVOO-L15, and LO-L15) stored for 15 days at 60 °C. The highest fluorescence peaks for the fresh edible oil samples are seen with $342 < \lambda_{ex} < 400$ nm and $403 < \lambda_{em} < 518$ nm for RO, $338 < \lambda_{ex} < 386$ nm and $408 < \lambda_{em} < 484$ nm for SO, $343 < \lambda_{ex} < 360$ nm and $514 < \lambda_{em} < 531$ nm for EVOO, and $340 < \lambda_{ex} < 356$ nm and $519 < \lambda_{em} < 542$ nm for LO; whereas the highest fluorescence peaks for the uncapped edible oil samples are observed with $\lambda_{ex} = 349$ nm and $\lambda_{em} = 442$ nm for RO, $344 < \lambda_{ex} < 387$ nm and $414 < \lambda_{em} < 481$ nm for SO, $345 < \lambda_{ex} < 372$ nm and $512 < \lambda_{em} < 531$ nm for EVOO, and $340 < \lambda_{ex} < 356$ nm and $519 < \lambda_{em} < 542$ nm for LO.

The excitation and emission characteristics indicate that the fluorescence peaks arise from oxidation products, polyphenols, and tocopherols, which are expected to be present in edible vegetable oils. Indeed, the peak observed in the region $\lambda_{ex} = 300 – 400$ nm and $\lambda_{em} = 400 – 500$ nm (Figs 1b, c, d and e) was attributed to the oxidation products contained in vegetable oils (Tena et al., 2012). Some previous works reported that polyphenols can present peaks in the region of $\lambda_{ex} = 260 – 310$ nm and $\lambda_{em} = 310 – 370$ nm (Zandomeneghi, Carbonaro, & Caffarata, 2005; Ali et al., 2020). Moreover, the same peak may correspond to the tocopherols. But this attribution was considered to be erroneous according to Christensen et al., (2006). Actually, this component does not agree with the fluorescence characteristics of tocopherol found in the literature (Duggan, Bowman, Brodie, & Udenfriend, 1957). Recently,

it has been reported that the emission of some fluorescent components at 525 nm was not fully resolved and this fluorescent compound corresponds to the more than one chemical compound present in vegetable oil (Sikorska et al., 2019b).

3.2. Application of PARAFAC on excitation-emission matrix obtained from edible vegetable oils during oil aging at 60 °C

As shown in **Fig. S1a and 1b**, the presence of the massive band of peaks (in the dashed circle) in the place of the first Rayleigh scatter is the result of masking the 1st and 2nd Rayleigh scatter options available on the Fluoromax-4 spectrofluorimeter. For the edible oil data set, non-trilinear parts were removed by using EEM filter (**Fig. S2a and 2b**) or flucut function. An attempt was performed by removing the top part of the 3D spectra which is > 9.2*1e^{6} CPS) and replacing it with NaN but no reliable model was obtained.

To resolve the profile of fluorophores in edible oils during storage, PARAFAC was applied to the raw EEM to fit the array. Two, three, four, five components models were performed. The explained variance for each number of components is given in **Table 1.** The relative change in explained variances increases from 1 to 5 components model. Although the 4 and 5 components models exhibited the highest percentage of explained variance, only the 3 components model obtained the highest scores of similarity measure of splits (83.8 %) and the highest number of components. Therefore, the split-half analysis and investigation of residuals suggested that the evolution of edible vegetable oils EEM fluorescence spectra during their storage were best-fitted by a three-component model (**Table 1**). This model exhibited the optimal value of the number of components, explained variance and similarity measure of splits. Sikorska et al., (2019b) reported an optimal PARAFAC model with four

components (explained variance 99.1 %, core consistency value 70) during investigating the EEMs of different RO samples during storage. The authors used core consistency and a visual inspection of both the residuals and the loadings to validate their model.

Fig. 2 provides the split-half model estimates for all three components in the emission and excitation modes, respectively. It is noticeable that the spectra were very similar to each other and had the same peak positions, from which it can be concluded that the three-component PARAFAC model is appropriate for edible oil samples studied in the present case.

Fig. 3 shows the emission (a) and excitation (b) spectra of three components present in edible vegetable oil samples obtained through the decomposition of the EEM spectra using the three component PARAFAC models. These two modes, emission and excitation spectra, were the same for the four edible oils studied despite the difference of their EEM profile and represented the underlying pure spectra of fluorophores characteristic of RO, SO, LO, and EVOO samples during 15 days of storage at 60 °C. The first mode of the PARAFAC model contained information about the specific concentration of these fluorophores in every measured edible oil samples. The estimated excitation spectra presented maxima at 395 nm (component 1), 344 nm (component 2) and 355 nm (component 3) (**Fig. 3b**). This trend corresponds to the peaks in the raw fluorescence landscapes (**Fig. S1**). While their corresponding estimated emission spectra exhibit their maxima at 487 nm, 420 nm and 528 nm, respectively (**Fig. 3a**).

The pair of excitation/emission wavelength (395/487 nm) corresponds to the maximum fluorescent intensity of the first component. According to previous findings, these spectra are similar to those of oxidation products (Guimet et al., 2005). An intensive band in the range 450 – 650 nm was attributed to the oxidation products while studying chemical changes of

313 thermo-oxidized virgin olive oil (Tena, Garcia-Gonzalez, & Aparicio, 2009; Tena et al.,
314 2012). Based on these findings, the first component can be assigned to secondary oxidation
315 products such as ketones, aldehydes and other carbonyl compounds in agreement with the
316 findings of Guimet et al., (2005).
317 The second pair of excitation/emission wavelength (344/420 nm) corresponds to the
318 maximum fluorescent intensity of the second component. Rodriguez Delgado, Malovana,
319 Perez, Borges, & Garcia Montelongo (2001) reported that phenolic compounds show
320 maximum excitation between 265 and 335 nm, and maximum emission in the 358 - 426 nm
321 range. Although the maximum emission (420 nm) of this excitation/emission wavelength is
322 comprised between 358 and 426 nm, its maximum excitation (344 nm) is not included
323 between 265 and 335 nm. Again, according to Guimet et al., (2005), oils at early degradation
324 stages exhibit strong fluorescence between λ_{ex} = 315 – 370 nm; λ_{em} = 415 – 460 nm.
325 Moreover, this component, which was ascribed to compounds formed during cold-pressed
326 rapeseed oil oxidation, appeared at 320/420 nm in excitation/emission (Sikorska et al.,
327 2019b). In accordance with those findings, the second component could be hypothesized to
328 correspond to primary oxidation compounds, such as conjugated hydroperoxides (Guimet et
329 al., 2005), present in edible oil samples.
330 The third pair of excitation/emission (355/528 nm) corresponds to the maximum fluorescent
331 intensity of the third component. Despite several identification attempts, the assignment of
332 this component to its real chemical structure remained uncertain. Moreover, the spectral
333 ranges of excitation between 300 and 400 nm and emission between 400 and 695 included
334 chlorophylls, which peak is used to be much more intense than those of other components
335 (Guimet, Ferré, Boqué, & Rius, 2004; Guimet et al., 2005). However, the peak is usually
336 detected at 695 nm (Guimet, 2005), but has already been detected at 681 nm (Kyriakidis &
337 Skarkalis, 2000), and even at 668 nm (Christensen et al., 2006; Sikorskaet al., 2019a). These

wavelengths are outside of the range of emission wavelength fixed in the present study to such an extent that this hypothesis can be excluded. As it was previously reported, the peak at λ_{em} = 525 nm was also attributed to vitamin E from EVOO (Guimet et al., 2004). This hypothesis was confirmed by the same authors who observed an increase in the fluorescent intensity at 525 nm after the addition of vitamin E to EVOO. Previously, the same experiment has already been performed to attempt the same peak identification (Kyriakidis & Skarkalis, 2000). However, Christensen et al., (2005) reported that this component was erroneously assigned to tocopherol based on the results obtained by Kyriakidis and Skarkalis (2000). Recently, the pair of excitation/emission corresponding to 360/530 nm was considered as one of the components detected in studying the evolution of fluorescence of cold-pressed rapeseed oil during storage (Sikorska et al., 2019a). The authors found the origin of this component less obvious as well. The loading of its emission profile presented a similarity with the present profile which exhibits additional broad emission with low-intensity on the short-wavelength side. This was explained by the fact that the emission of some fluorescent components was not fully resolved, and therefore this component corresponded to more than one chemical.

The score of the model are estimates of the relative concentration of the three fluorophores in every edible oil samples identified by the loadings and are therefore measures of the amount of the fluorophores as shown in **Fig. 4**. Oil samples were grouped according to their botanical origins for easier interpretation. For every botanical group, the concentrations of the three components can be calculated. For example, it can be observed that the concentrations of the first and second components, corresponding hypothetically to primary and secondary oxidation products showed the following tendency RO > SO > EVOO > LO. Indeed, refined oils, namely RO and SO, exhibited the highest score of relative concentrations of both oxidation products compared with unrefined ones (EVOO and LO). This implies that the evolution of these oxidation compounds throughout the 15 days of storage depends on the

363 previous refining step undergone by the edible oils. This profile is, to our best knowledge the
364 first time, obtained with PARAFAC model. It is well known that refined oils are more reliable
365 to undergo oxidation processes when compared with unrefined oils (Guimet et al., 2004). The
366 main reason would be due to the refining process, which may decrease the natural
367 antioxidants (phenolic compounds, tocopherols and beta-carotene) contained in edible
368 vegetable oils.
369
370 Regarding the third component, the tendency showed the following order LO > EVOO > RO
371 > SO during the 15 days of storage. Unrefined oils are supposed to contain less natural
372 antioxidant compounds (vitamin E) since the refining process drastically decreased its
373 content. This tendency may be explained by the difference between vitamin E and/or its
374 derivative contents in both categories of edible oils. Regarding the profile of tocopherol, the
375 order is in agreement with the contents of (β + γ) tocopherols in the investigated oils which
376 values are approximatively 363 mg/kg, 281 mg/kg, and 25.2 mg/kg for cold-pressed LO,
377 refined RO, and refined SO, respectively (Gliszczyńska-Świgło, Sikorska, Khmelinskii, &
378 Sikorski, 2007). The value for EVOO (12.3 mg/Kg) is normally the lowest between the four
379 edible oils studied; however, the presence of the important peak corresponding to chlorophyll
380 close to 525 nm may interfere and could present an impact in the increase of fluorescence
381 intensity of EVOO at this wavelength. In fact, only EEM of EVOO presented an increase of
382 fluorescence intensity between 625 and 650 nm that should correspond to the beginning or the
383 tail of the chlorophyll's peak. Guimet (2005) has already reported that, in EVOOs, the
384 chlorophyll peak was much more intense than those of the other fluorescent molecules and
385 can influence strongly the fluorescence intensity of the peak at 525 nm. Consequently, the
386 different magnitude of this peak may cause problems when handling the data and, for this
387 reason, the fluorescent region of chlorophylls has been often removed.

388

389 The contributions of each of the three PARAFAC components were shown in **Fig. 5 (a-l).**
390 The score values obtained in the PARAFAC decomposition were plotted against the storage
391 time to explore the impact of thermo-oxidation throughout the storage period. The systematic
392 variations of the score values, corresponding to the respective components were observed
393 except for component 1 for LO and component 3 for SO. Regarding the evolution of
394 oxidation products, RO showed a decrease of primary products during storage (**Fig. 5a**) while
395 the secondary products showed the highest score at 9 days of storage for capped samples and
396 decreased until the 13^{th} day for uncapped ones (**Fig. 5b**). For EVOO samples (**Fig. 5c-d**), the
397 primary oxidation products reached the highest score on day 9 for capped samples and only
398 on day 6 for uncapped ones, while the secondary products exhibited a progressive increase
399 during 15 days of storage. For LO samples (**Fig. 5e-f**), the primary oxidation products
400 progressed in a less systematic way for capped and uncapped samples; however, no
401 compounds were detected before 13 days for both storage conditions. It is probably due to the
402 fact that LO samples were the freshest among the four studied oils. For SO, **Fig. 5g** shows a
403 slight decrease of component 2 during storage but the highest score of component 1 was
404 reached at 3 days for capped and uncapped samples (**Fig. 5h**).
405 Regarding vitamin E (tocopherols), **Fig. 5i-j** showed a systematic and slight decrease for RO
406 and EVOO during storage, while the level of vitamin E in LO samples remained stable
407 throughout storage (**Fig. 5k**). The most spectacular diminution was observed with SO
408 reaching the lowest score after 9 days of storage (**Fig. 5l**). It can be attributed to the fact that
409 SO was a refined oil and contained the lowest value of tocopherols it seems that these
410 tocopherols were more thermosensitive.
411

412 **4. Conclusion**

This study aimed to investigate the potential of fluorescence spectroscopy coupled with PARAFAC for monitoring the thermo-oxidation at 60 °C, in the frame of the Schaal oven test, undergone by RO, SO, EVOO and LO samples during 15 days. The PARAFAC applied to fluorescence excitation-emission matrix scanned on RO, SO, EVOO, and LO samples separated three fluorophores components, which had different progression dynamics throughout storage. The results revealed, for the first time, the complexity of interpretation when PARAFAC is applied on EEM obtained from four oil fluorescence data sets. Indeed, the application of PARAFAC as multiway analysis method allowed to: (i) comprehend the evolution of primary and secondary oxidation products during storage; (ii) monitor the thermo-oxidation effect on the evolution of vitamin E depending on the refining process during their aging time; and iii) study a large number of edible oils including LO, with different profiles of mono-unsaturated and poly-unsaturated fatty acids, tocopherols, and chlorophylls.

Declaration of competing interest

The authors declare that they have no known competing financial interests or personal relationships that could have appeared to influence the work reported in this paper.

Acknowledgements

This work has been carried out in the framework of Alibiotech project, which is financed by the European Union, the French State and the French Region of Hauts-de-France. The authors gratefully acknowledge the financial support from the Major Domain of Interest (DIM) "Eco-Energy Efficiency" of Artois University.

References

Ali, H., Iqbal, M.A., Atta, B.M., Ullah, R., & Khan, M.B. (2020). Phenolic profile and thermal stability of monovarietal extra virgin olive olive oils based on synchronous fluorescence spectroscopy. *Journal of Fluorescence*, 30, 939-947.

Andersen, C.M., & Bro, R. (2003). Practical aspects of PARAFAC modeling of fluorescence excitation-emission data. *Journal of Chemometrics*, 17, 200-215.

Botosoa, E.P., Chèné, C., Karoui, R. (2013a). Monitoring changes in sponge cakes during aging by front face fluorescence spectroscopy and instrumental techniques. *Journal of Agricultural and Food Chemistry*, 61, 2686-2695.

Botosoa, E.P., Chèné, C., & Karoui, R. (2013b). Use of front face fluorescence for monitoring lipid oxidation during ageing of cakes. *Food Chemistry*, 141, 1130-1139.

Bro, R. (1999). Explorative study of sugar production using fluorescence spectroscopy and PARAFAC analysis. *Chemometrics and Intelligent Laboratory System*, 46, 133-147.

Christensen, J., Miquel Becker, E., & Frederiksen, C.S. (2005). Fluorescence spectroscopy and PARAFAC in the analysis of yogurt. *Chemometrics and Intelligent Laboratory System*, 75, 201-208.

Christensen, J., Nørgaard, L., Bro, R., & Engelsen, S.B. (2006). Multivariate autofluorescence of intact food systems. *Chemical Reviews*, 106, 1979-1994.

Cordella, C.B.Y., Tekye, T., Rutledge, D.N., & Leardi, R. (2012). A multiway chemometric and kinetic study for evaluating the thermal stability of edible oils by ^{1}H NMR analysis: Comparison of methods. *Talanta,* 88, 358-368.

Cuvelier, M.E., & Maillard, M.N. (2012). Stabilité des huiles alimentaires au cours de leur stockage. *Oilseeds & fats Crops and Lipids*, 19, 125-132.

461 Domínguez Manzano, J., Muñoz de la Peña, A., & Durán Merás, I. (2019). Front-face
462 fluorescence combined with second-order multiway classification, based on
463 polyphenol and chlorophyll compounds, for virgin olive oil monitoring under different
464 photo- and thermal-oxidation procedures. *Food Analytical Methods*, 12, 1399-1411.
465 Duggan, D.E., Bowman, R.L., Brodie, B.B., & Udenfriend, S. (1957). A
466 spectrophotofluorometric study of compounds of biological interest. *Archives of*
467 *Biochemistry and Biophysics*, 68, 1-14.
468 Dugo, G., Rotondo, A., Mallamace, D., Cicero, N., Salvo, A., Rotondo, E., & Corsaro, C.
469 (2015). Enhanced detection of aldehydes in extra-virgin olive oil by means of band
470 selective NMR spectroscopy. *Physica A*, 420, 258-264.
471 El-Hamidi, M., & Zaher, F. (2018). Production of vegetable oils in the world and in Egypt: an
472 overview. *Bulletin of the National Research Centre,* 42:19,
473 https://doi.org/10.1186/s42269-018-0019-0.
474 Gliszczyńska-Świgło, A., Sikorska, E., Khmelinskii, I., & Sikorski, M. (2007). Tocopherol
475 content in edible plant oils. *Polish Journal of Food and Nutrition Sciences*, 57, 157-
476 161.
477 Gredilla, A., Fdez-Ortiz de Vallejuelo, S., Elejoste, N., de Diego, A., & Madariaga, J.M.
478 (2016). Non-destructive spectroscopy combined with chemometrics as a tool fro green
479 chemical analysis of environmental samples: a review. *Trends in Analytical*
480 *Chemistry*, 76, 30-39.
481 Guimet, F. Olive oil characterization using excitation-emission fluorescence spectroscopy and
482 three-way methods of analysis, Doctoral Thesis, Taragona, 2005.
483 Guimet, F., Ferré, J., Boqué, R., & Rius, F.X. (2004). Application of unfold principal
484 component analysis and parallel factor analysis to the exploratory analysis of olive oils

485 by means of excitation-emission matrix fluorescence spectroscopy. *Analytica Chimica*
486 *Acta*, 515, 75-85.
487 Guimet, F., Ferré, J., Boqué, R., Vidal, M., & Garcia, J. (2005). Excitation-emission
488 fluorescence spectroscopy combined with three-way methods of analysis as a
489 complementary technique for olive oil characterization. *Journal of Agricultural and*
490 *Food Chemistry*, 53, 9319-9328.
491 Hassoun, A., & Karoui, R. (2016). Monitoring changes in whiting (*Merlangius merlangus*)
492 fillets stored under modified atmosphere packaging by front face fluorescence
493 spectroscopy and instrumental techniques. *Food Chemistry,* 200, 343–353.
494 Karoui, R., Cartaud, G., & Dufour, E. (2006). Front-face fluorescence spectroscopy as a rapid
495 and nondestructive tool for differentiating various cereal products: A preliminary
496 investigation. *Journal of Agricultural and Food Chemistry, 54,* 2027–2034.
497 Karoui, R., Hammami, M., Rouissi, H., & Blecker, C. (2011). Mid infrared and fluorescence
498 spectroscopies coupled with factorial discriminant analysis technique to identify sheep
499 milk from different feeding systems. *Food Chemistry,* 127, 743–748.
500 Karoui, R., Nicolaï, B., & De Baerdemaeker, J. (2008). Monitoring the egg freshness during
501 storage under modified atmosphere by fluorescence spectroscopy. *Food and*
502 *Bioprocess Technology, 1,* 346–356.
503 Kyriakidis, N.B., & Skarkalis, P. (2000). Fluorescence spectra measurement of olive oil and
504 other vegetable oils. *Journal of AOAC International*, 83, 1435-1439.
505 Moller, J.K.S., Parolari, G., Gabba, L., Christensen, J., & Skibsted, L.H. (2003) *Journal of*
506 *Agricultural and Food Chemistry,* 51, 1224-1230.
507 Pedersen, D.K., Munck, L., & Engelsen, S.B. (2002). Screening for dioxin contamination in
508 fish oil by PARAFAC and N-PLSR analysis of fluorescence landscapes. *Journal of*
509 *Chemometrics*, 16, 451-460.

510 Qi, B., Zhang, Q., Sui, X., Wang, Z., Li, Y., & Jiang, L. (2016). Differential scanning
511 calorimetry study – Assessing the influence of composition of vegetable oils on
512 oxidation. *Food Chemistry*, 194, 601-607.
513 Rodriguez Delgado, M.A., Malovana, S., Perez, J.P., Borges, T., & Garcia Montelongo, F.J.
514 (2001). Separation of phenolic compounds by high-performance liquid
515 chromatography with absorbance and fluorimetric detection. *Journal of*
516 *Chromatography A*, 912, 249-257.
517 Saleem, M., Ahmad, N., Ullah, R., Ali, Z., Mahmood, S., & Ali, H. (2020). Raman
518 spectroscopy-based characterization of canola oil. *Food Analytical Methods*, 13, 1292-
519 1303.
520 Saleem, M., Ahmad, N., Ali, H., Bilal, M., Khan, S., Ullah, R., Ahmed, M., & Mahmood, S.
521 (2017). Investigating temperature effects on extra virgin olive oil using fluorescence
522 spectroscopy. *Laser Physics*, 27, 125602.
523 Schaich, K.M. (2013). Challenges in elucidating lipid oxidation mechanisms - When, where
524 and how do products arise? in: A. Logan, U. Nienaber, X. S. Pan (Eds.), Lipid
525 oxidation challenges in food systems, AOCS press, Urbana, pp. 1-52.
526 Sikorska, E., Khmelinskii, I., & Sikorski, M. (2019a). Fluorescence spectroscopy and imaging
527 instruments for food quality evaluation, in: J. Zhong, X. Wang (Eds), Evaluation
528 Technologies for Food Quality, Woodhead Publishing Series, Duxford, pp. 491-533.
529 Sikorska, E., Wójcicki, K., Kozak, W., Gliszczyńska-Świgło, A., Khmelinskii, I., Górecki, T.,
530 Caponio, F., Paradiso, V.M., Summo, C., & Pasqualone, A. (2019b). Front-face
531 fluorescence spectroscopy and chemometrics for quality control of cold-pressed
532 rapeseed oil during storage. *Foods*, 665, 1-16 doi:10.3390/foods8120665.

533 Tena, N., Aparicio, R., & García-González, D.L. (2012). Chemical changes of thermoxidized
534 virgin olive oil determined by excitation– emission fluorescence spectroscopy (EEFS).
535 *Food Research Internation*, 45, 103-108.
536 Tena, N., Garcia-Gonzalez, D.L., & Aparicio, R. (2009). Evaluation of virgin olive oil
537 thermal deterioration by fluorescence spectroscopy. *Journal of Agricultural and Food*
538 *Chemistry,* 57, 10505-10511.
539 Ullah, R., Khan, S., Bilal, M., Ali, H., & Khalil, U. (2019). Comparison among different
540 postharvest ripening treatment based on carotene contents in mango using UV-Vis and
541 Raman spectroscopy. *Laser Physics*, 29, 105701.
542 Ullah, R., Khan, S., Shah, A., Ali, H., & Bilal, M. (2018). Time-temperature dependent
543 variations in beta-carotene contents in carrot using different spectrophotometric
544 techniques. *Laser Physics*, 28, 055601.
545 Warner, K., Frankel, E. N., & Mounts, T. L. (1989). Flavor and oxidative stability of soybean,
546 sunflower and low erucic acid *Journal of the American Oil Chemists' Soc*iety, 66, 558-
547 564.
548 Zandomeneghi, M., Carbonaro, L., & Caffarata, C. (2005). Fluorescence of vegetable oils:
549 olive oils. *Journal of Agricultural and Food Chemistry,* 53, 759-766.
550
551
552
553

554 **List of Tables:**

555

556 **Table 1:** Explained variance as a percentage *versus* the number of components for PARAFAC

557 models of the fluorescence data with 1-5 components

PLS Toolbox	Number of components				
	1	2	**3**	4	5
Explained variance (%)	95.4	97.5	**99.3**	99.5	99.317
Similarity measure of splits (%)	98.7	40.9	**83.8**	59.5	0.1

558

559

560

561 **Legend to the Figures:**

562

563 **Fig. 1** Excitation-emission matrix contour plots of rapeseed oil (RO), sunflower oil (SO),
564 extra virgin olive oil (EVOO) (a), and linseed oil (LO) stored up to 15 days at 60 °C in
565 capped (b, and c) and uncapped (d, and e) flasks

566

567 **Fig. 2** Result from a split-half analysis performed by dividing oil samples into random groups
568 with emission and excitation modes

569

570 **Fig. 3** Emission (a) and excitation (b) mode loading vectors obtained from the three
571 component PARAFAC model calculated on the EEMs of the 44 oil samples in the excitation
572 range of 280 – 400 nm and emission range of 300 - 650 nm. Component 1 (—), component 2
573 (– · – · –), and component 3 (– – –).

574

575 **Fig. 4** PARAFAC model concentration mode loadings for rapeseed oil (RO), extra virgin
576 olive oil (EVOO), linseed oil (LO), and sunflower oil (SO). Component 1 (—), component 2
577 (– · – · –), and component 3 (– – –).

578

579 **Fig. 5** Scores versus storage time (a – l): scores on component 1 (b, d, f, and h), scores on
580 component 2 (a, c, e, and g), and scores on component 3 (i, j, k, and l) for rapeseed oil (RO)
581 (a, b, and i), extra virgin olive oil (EVOO) (c, d, and j), and linseed oil (LO) (e, f, and k), and
582 sunflower oil (SO) (g, h, and i), stored under 60 °C during 15 days in capped (empty bar) and
583 uncapped (checkered bar) flasks.

584 **Figure 1a:**

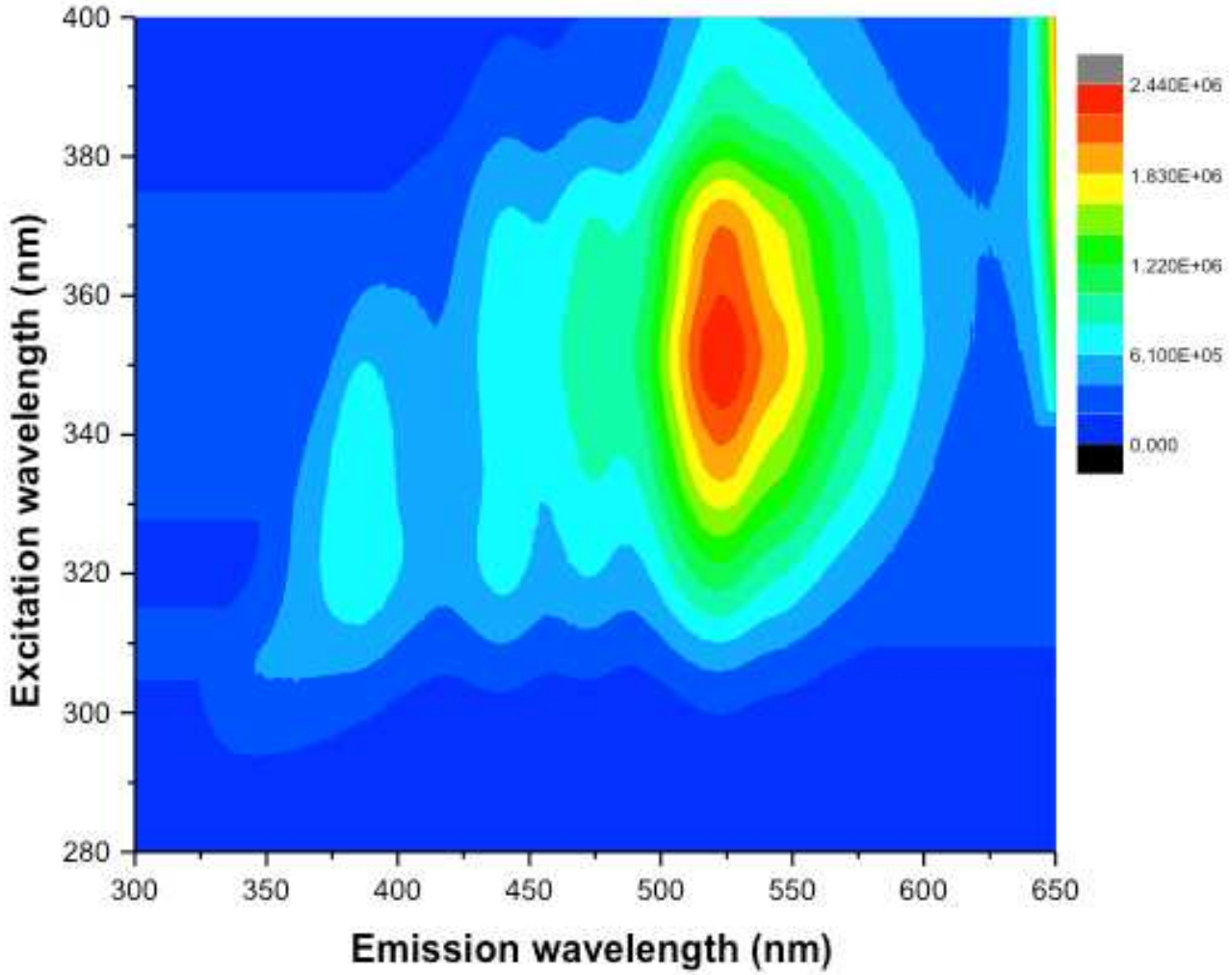

585

586

587 **Figure 1b:**

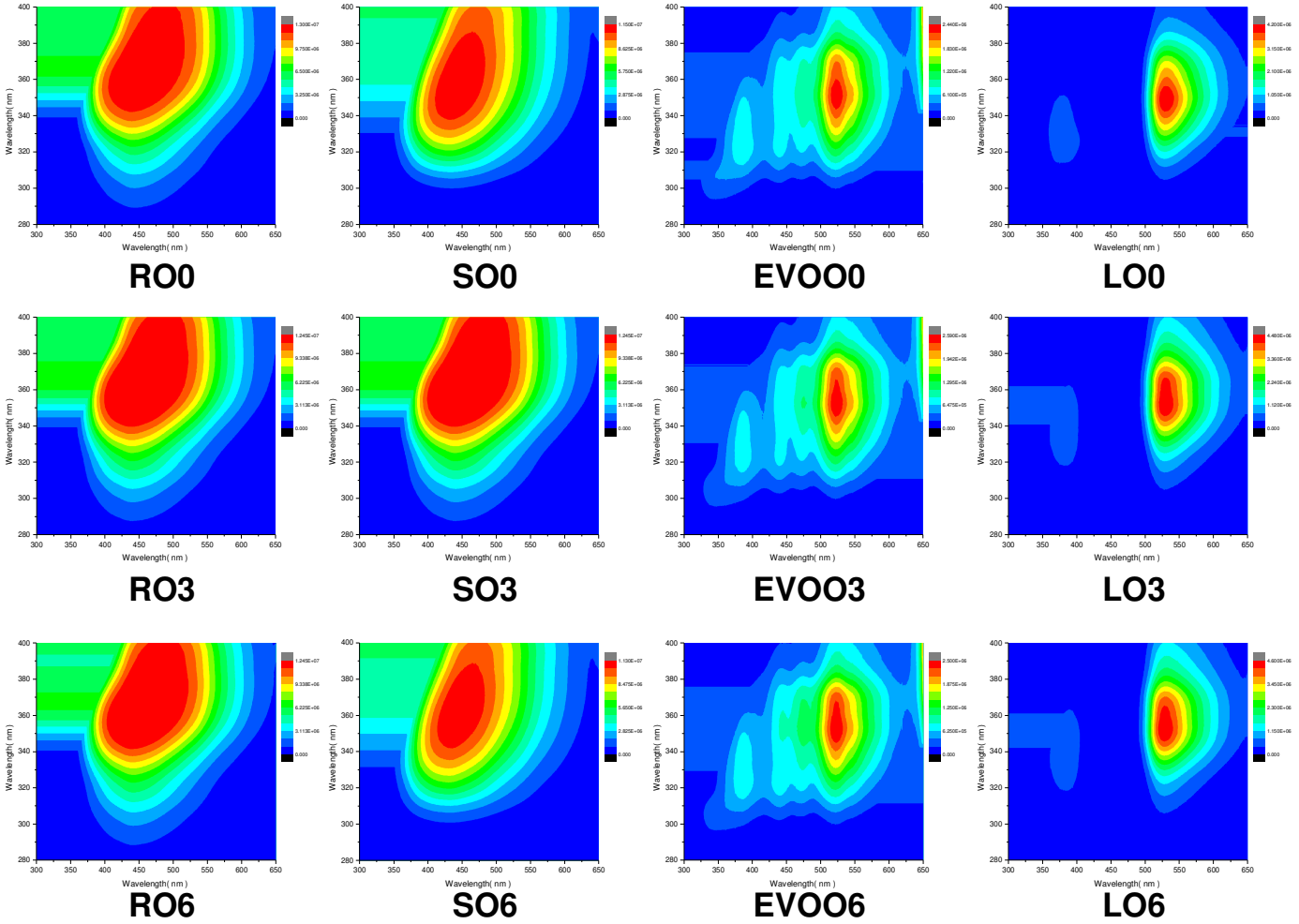

588

589

590 **Figure 1c:**

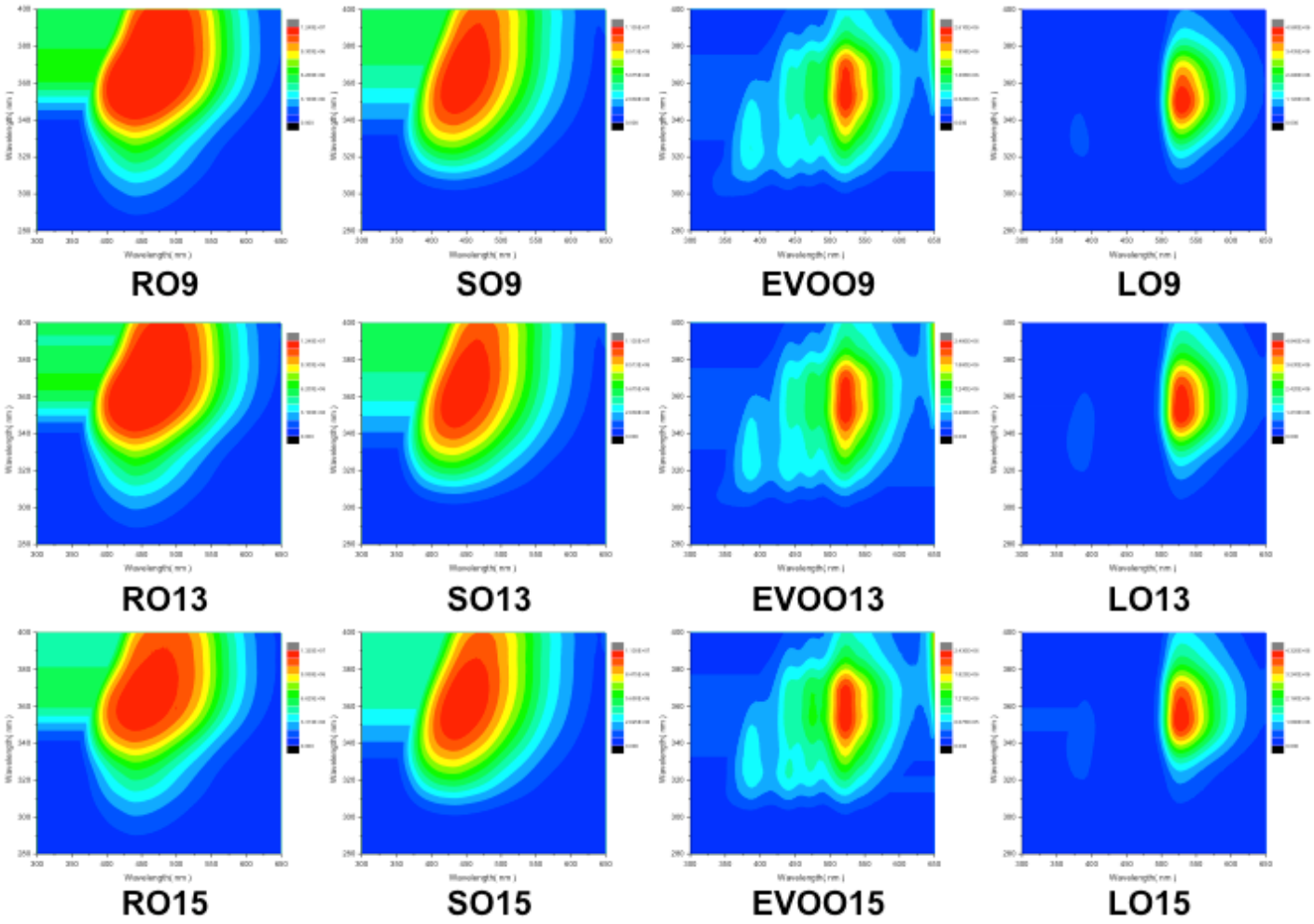

591

Figure 1d:

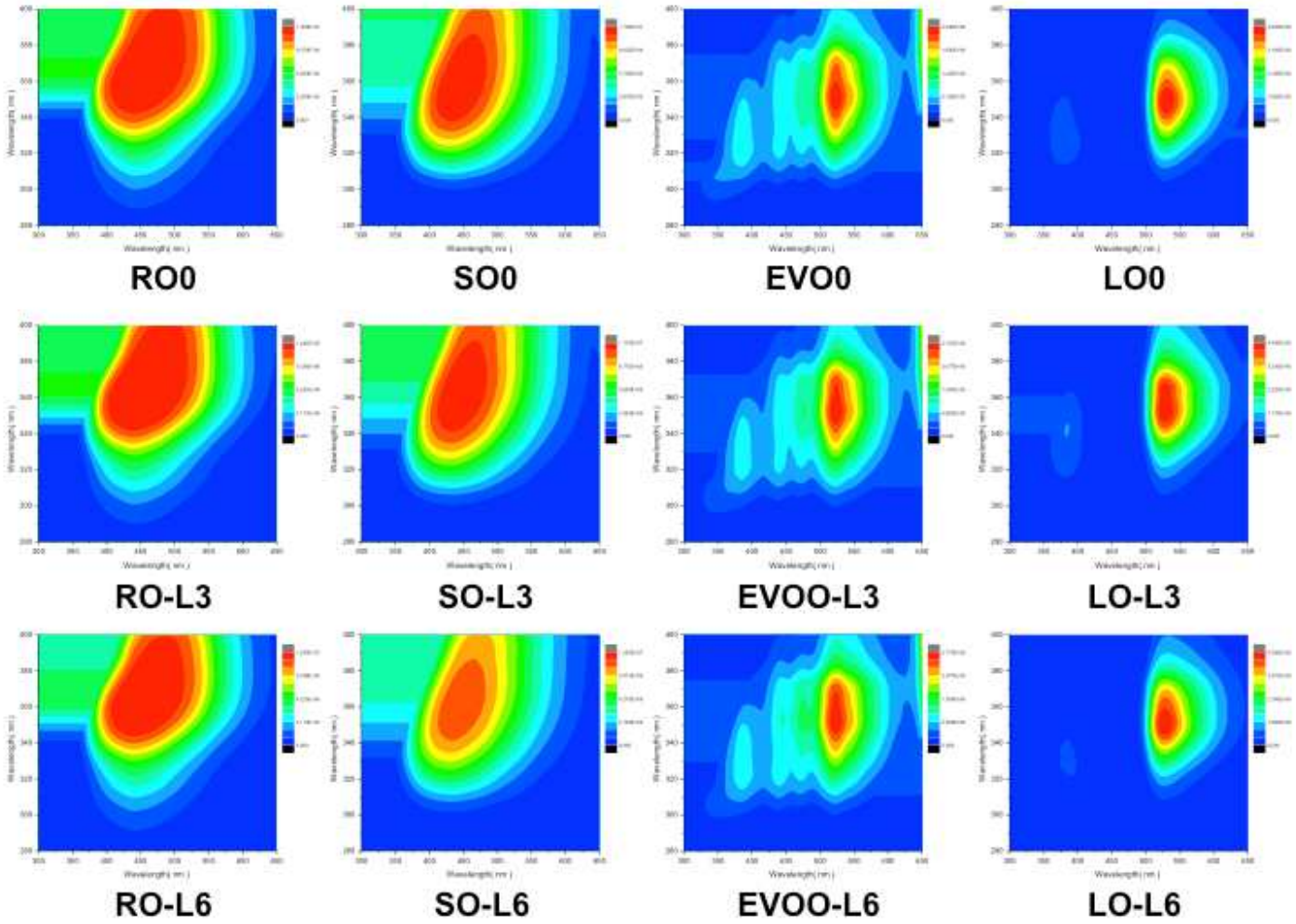

595

596 **Figure 1e:**

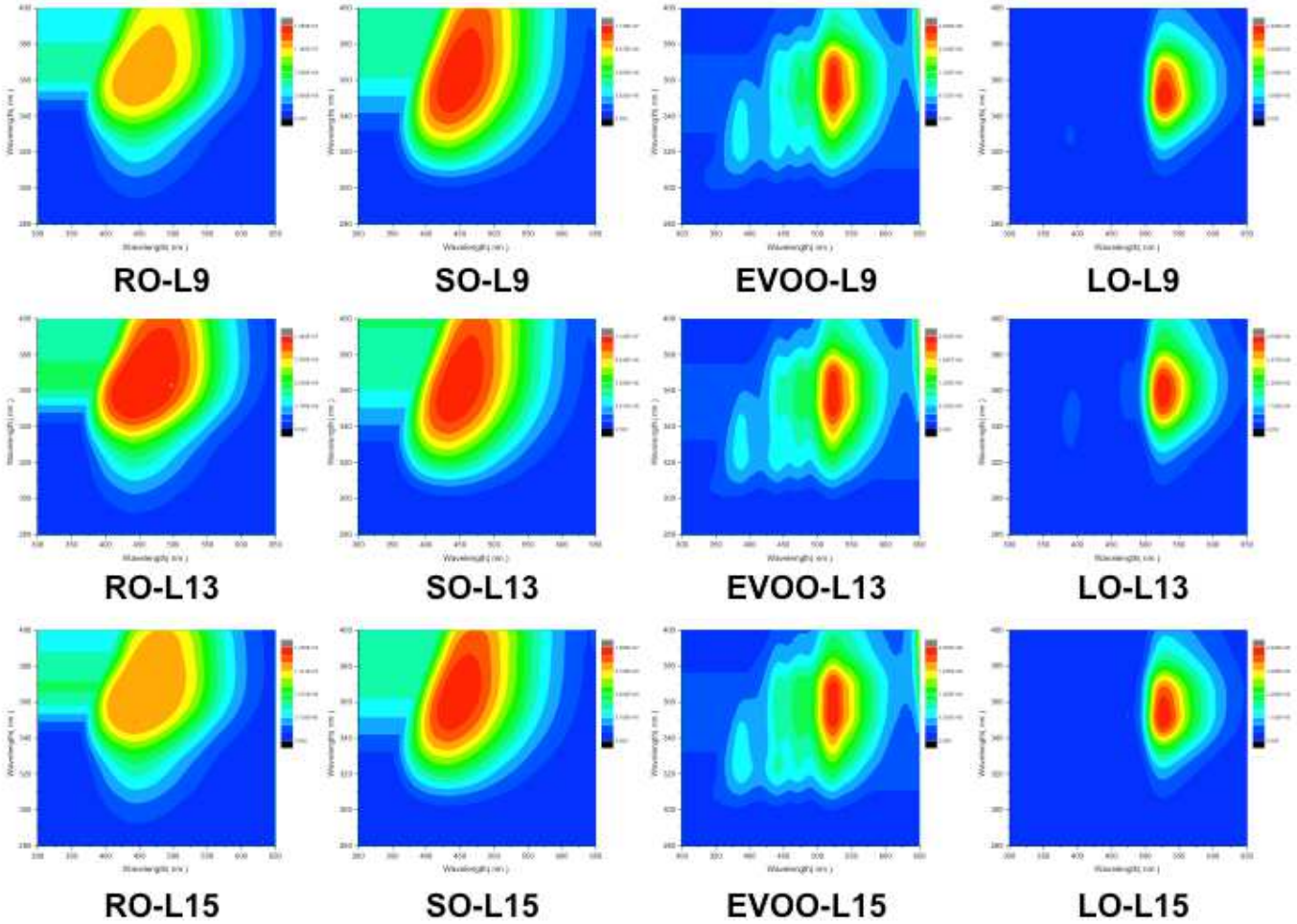

597

598 **Figure 2:**

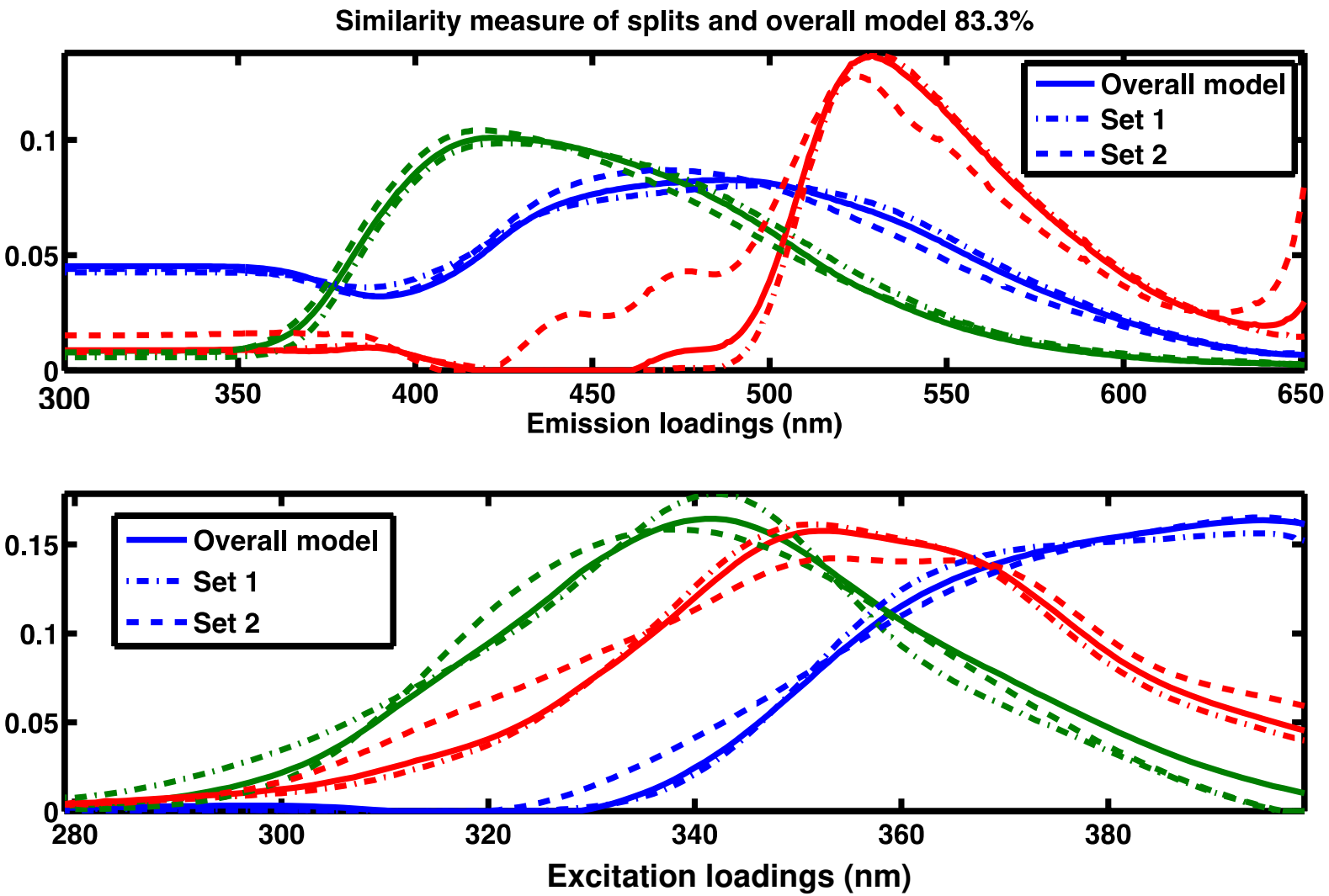

599

Figure 3a:

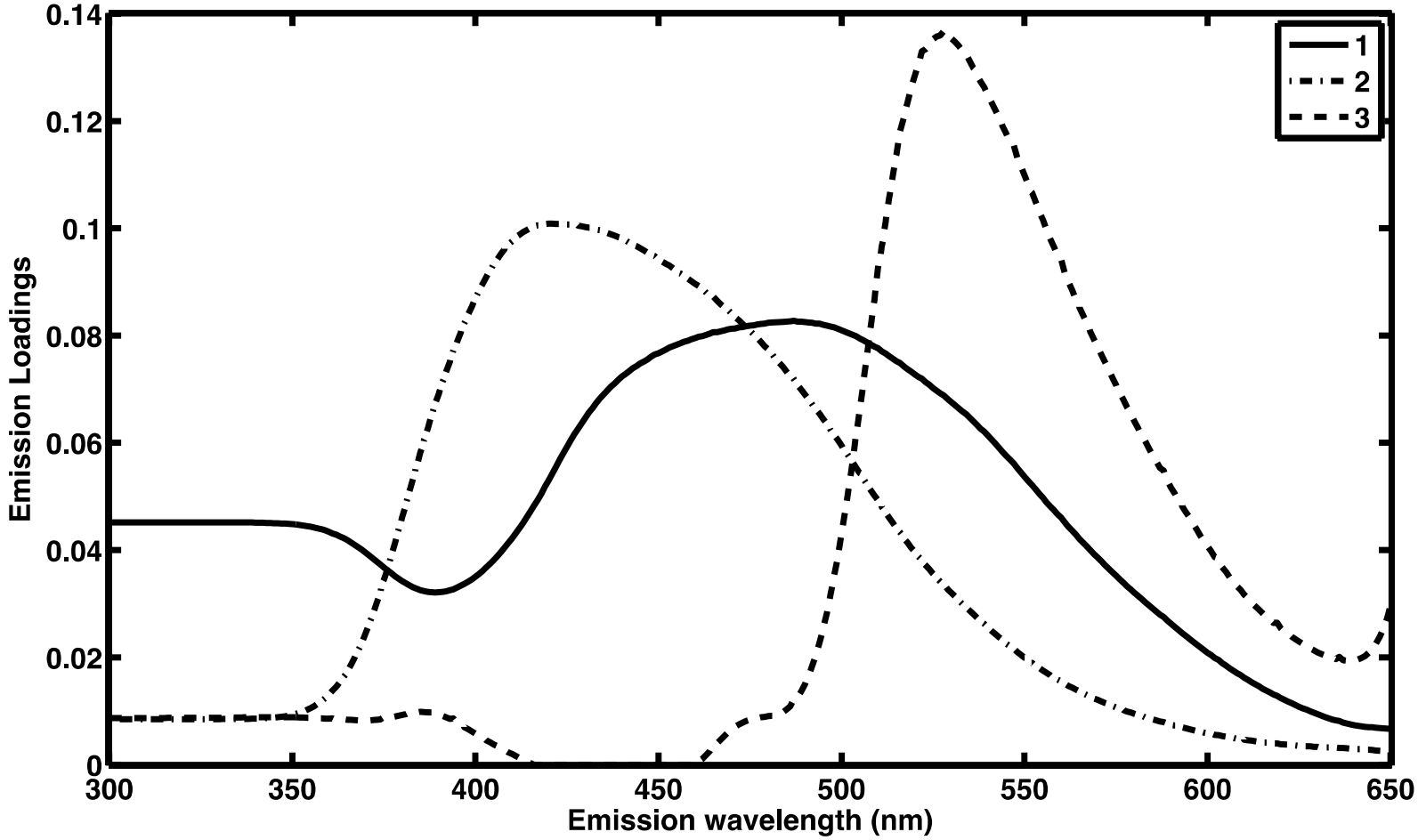
0.14
0.12
0.1
0.08
0.06
0.04
0.02
0
Emission Loadings
300
350
400
450
500
550
600
650
Emission wavelength (nm)
1
2
3

603 **Figure 3b:**

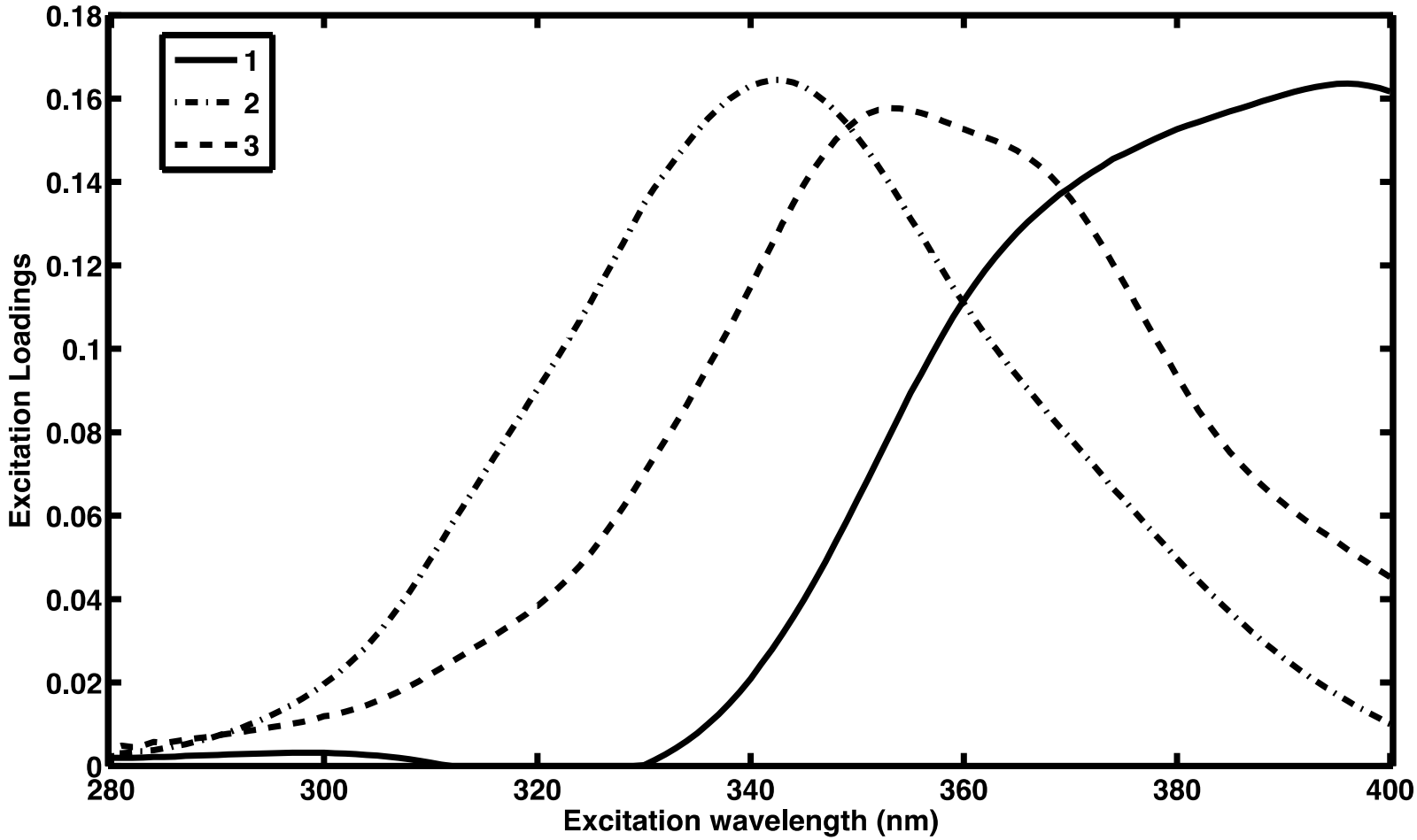

604

605

606 **Figure 4:**

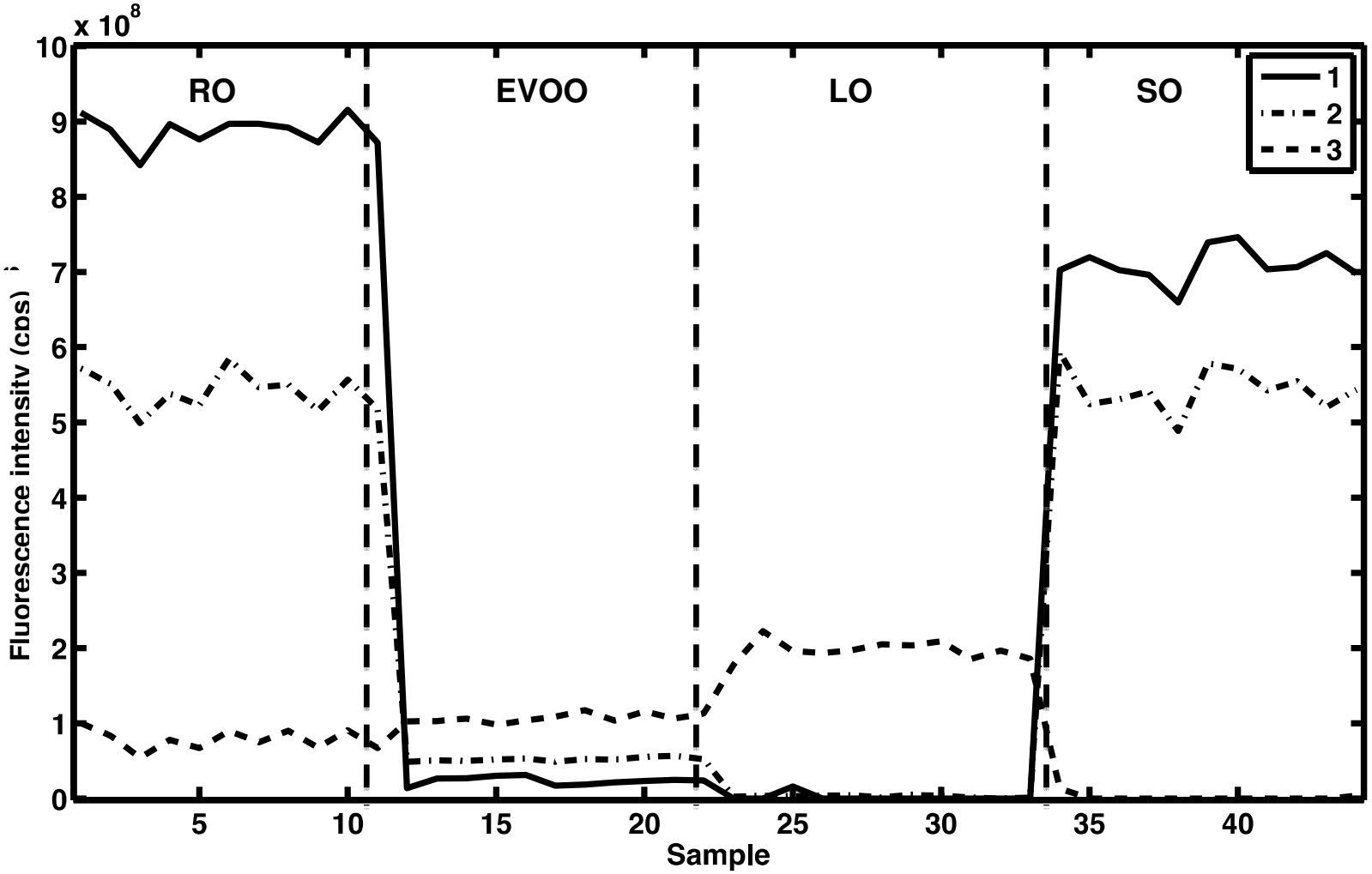

607

608 **Figure 5 (a – d):**

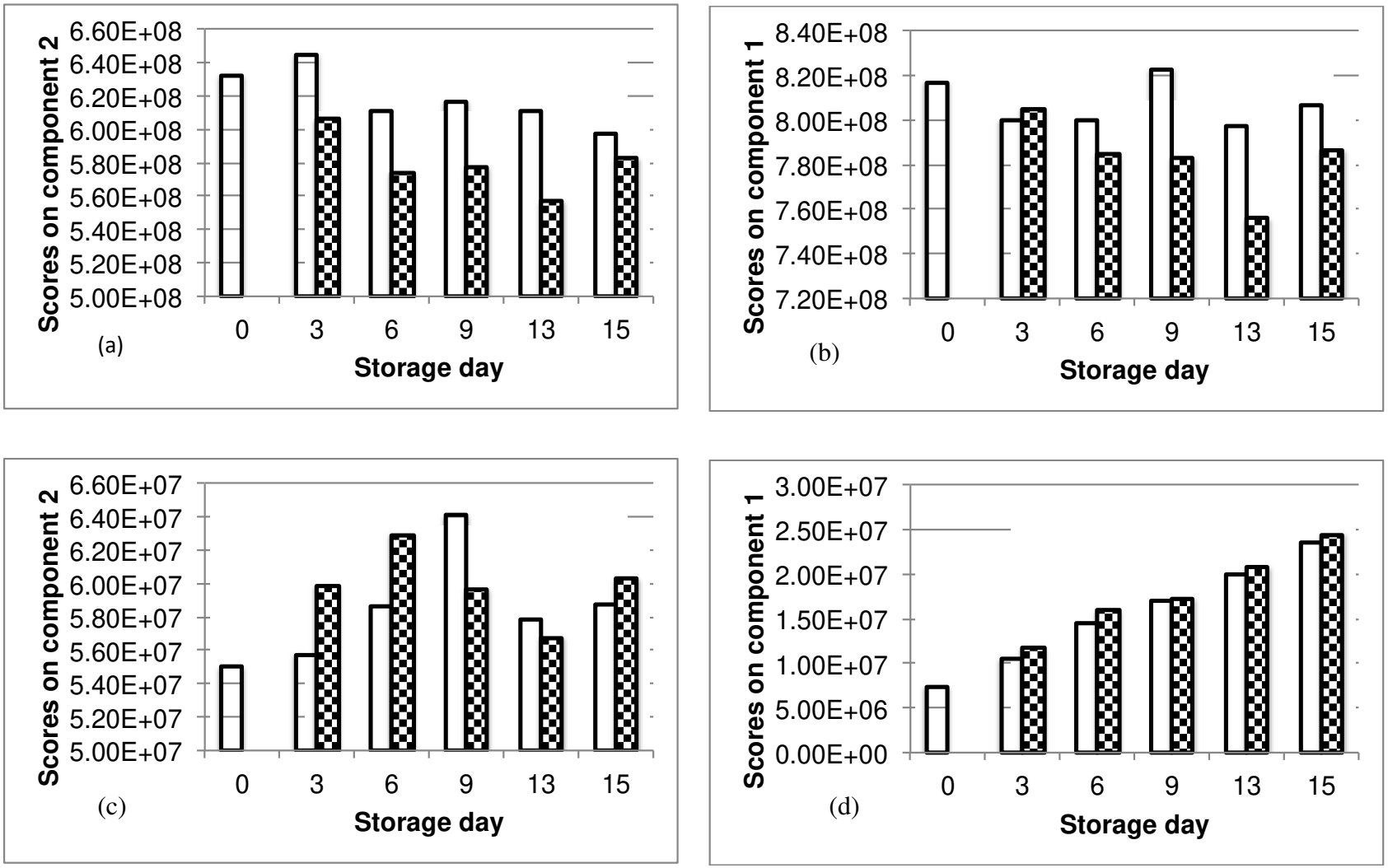

609

610

Figure 5 (e – h):

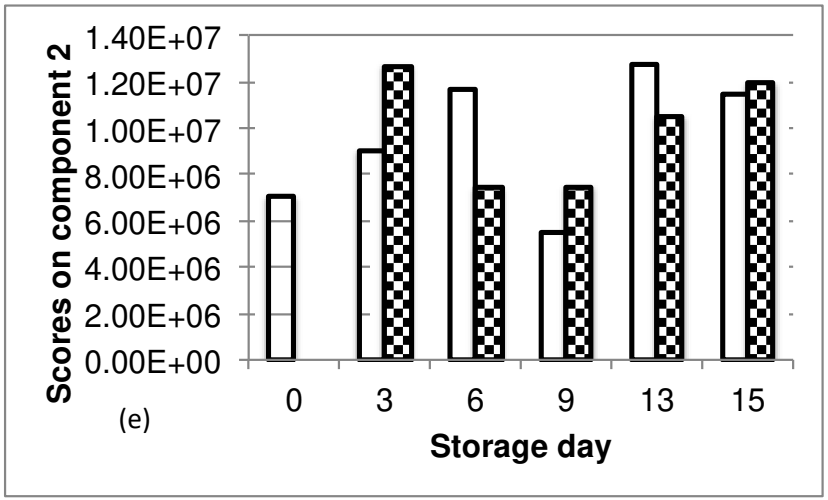
Scores on component 2
1.40E+07
1.20E+07
1.00E+07
8.00E+06
6.00E+06
4.00E+06
2.00E+06
0.00E+00
0
3
6
9
13
15
Storage day
(e)

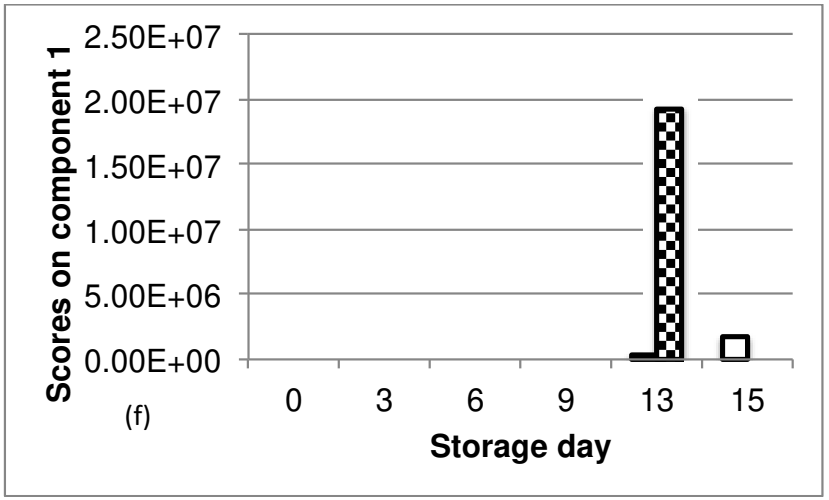
Scores on component 1
2.50E+07
2.00E+07
1.50E+07
1.00E+07
5.00E+06
0.00E+00
0
3
6
9
13
15
Storage day
(f)

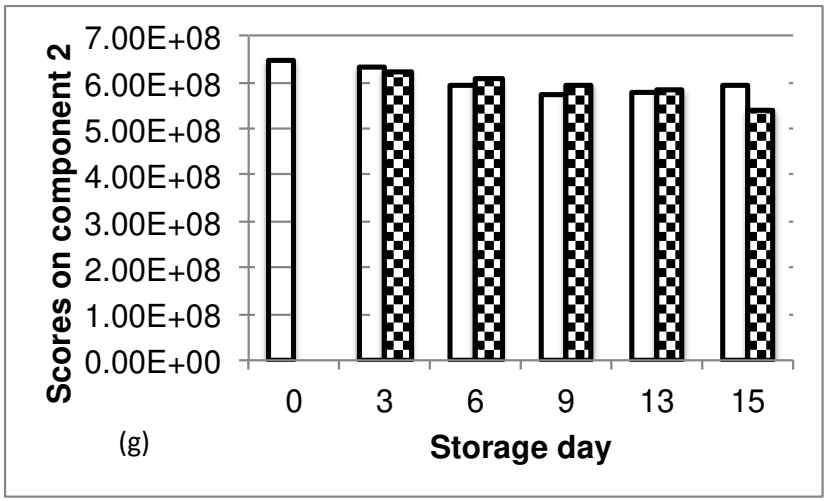
Scores on component 2
7.00E+08
6.00E+08
5.00E+08
4.00E+08
3.00E+08
2.00E+08
1.00E+08
0.00E+00
0
3
6
9
13
15
Storage day
(g)

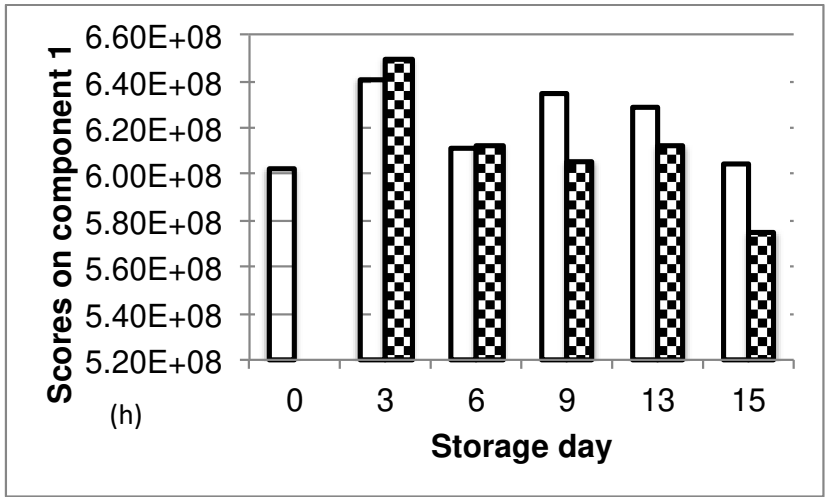
Scores on component 1
6.60E+08
6.40E+08
6.20E+08
6.00E+08
5.80E+08
5.60E+08
5.40E+08
5.20E+08
0
3
6
9
13
15
Storage day
(h)

Figure 5 (i – l):

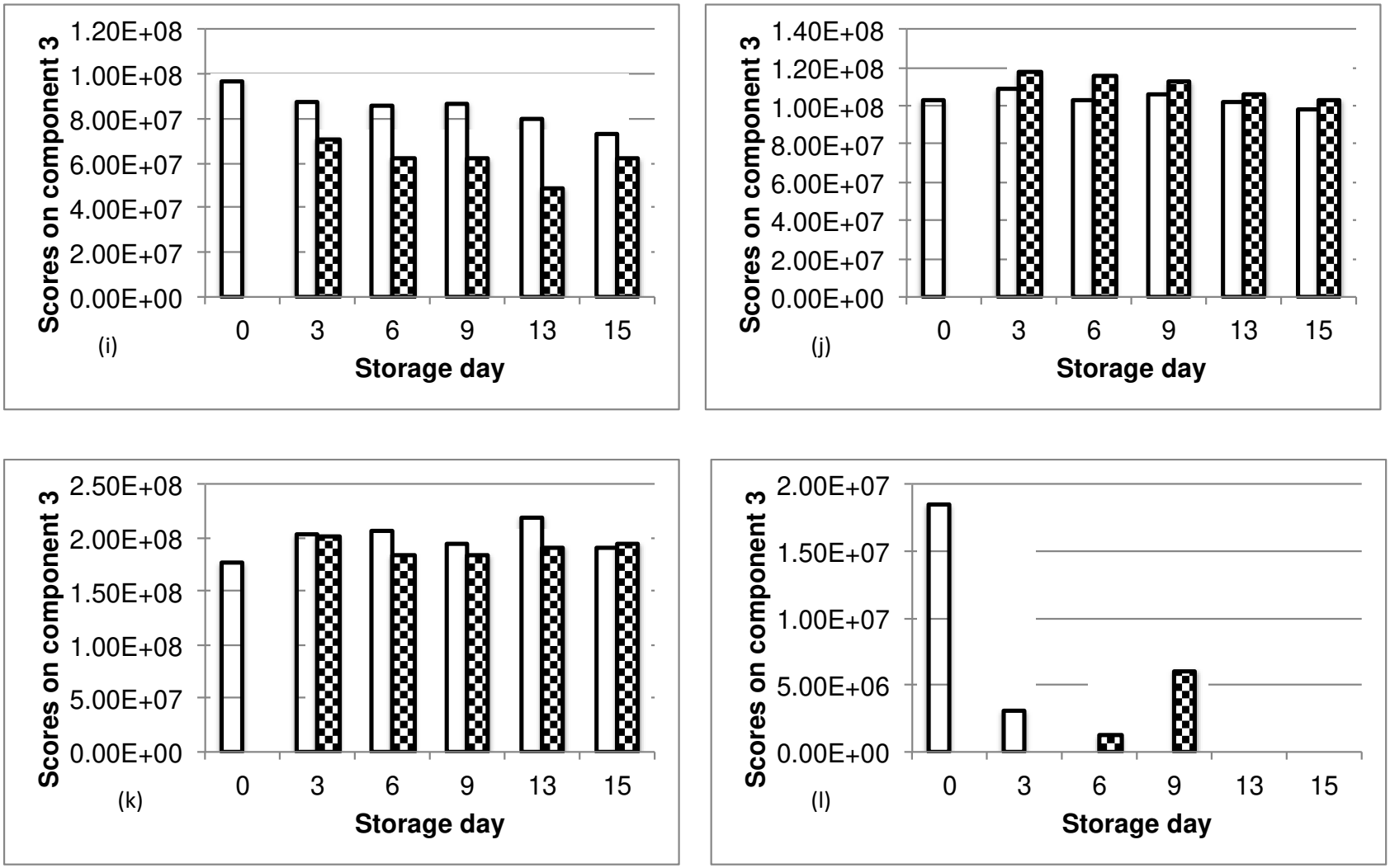
Scores on component 3
1.20E+08
1.00E+08
8.00E+07
6.00E+07
4.00E+07
2.00E+07
0.00E+00
0
3
6
9
13
15
Storage day
(i)
Scores on component 3
1.40E+08
1.20E+08
1.00E+08
8.00E+07
6.00E+07
4.00E+07
2.00E+07
0.00E+00
0
3
6
9
13
15
Storage day
(j)
Scores on component 3
2.50E+08
2.00E+08
1.50E+08
1.00E+08
5.00E+07
0.00E+00
0
3
6
9
13
15
Storage day
(k)
Scores on component 3
2.00E+07
1.50E+07
1.00E+07
5.00E+06
0.00E+00
0
3
6
9
13
15
Storage day
(l)